

The Dynamical Dipole Mode in Dissipative Heavy Ion Collisions

V.Baran^{1,2}, M.Cabibbo^{1,3}, M.Colonna¹, M.Di Toro¹, and N.Tsoneva⁴

¹ *Laboratorio Nazionale del Sud, Via S. Sofia 44, I-95123 Catania, Italy*

and University of Catania

² *NIPNE, Bucharest, Romania*

³ *CEA-SACLAY, France*

⁴ *INRNE, Sofia, Bulgaria*

(November 1, 2018)

Abstract

We study the effect of a direct Giant Dipole Resonance (*GDR*) excitation in intermediate dinuclear systems with exotic shape and charge distributions formed in charge asymmetric fusion entrance channels. A related enhancement of the *GDR* gamma yield in the evaporation cascade of the fused nucleus is expected. The dynamical origin of such *GDR* extra strength will show up in a characteristic anisotropy of the dipole gamma-emission. A fully microscopic analysis of the fusion dynamics is performed with quantitative predictions of the *GDR* photon yield based on a dynamics- statistics coupling model. In particular we focus our attention on the energy and mass dependence of the effect. We suggest a series of new experiments, in particular some optimal entrance channel conditions. We stress the importance of using the new available radioactive beams.

PACS: 24.30.Cz, 25.70.Jj, 25.70.Lm, 25.60.Pj

I. INTRODUCTION

The isovector giant dipole resonance represents a well established collective motion of finite nuclei extensively studied since more than fifty years [1]. The dependence on the nuclear structure of the reference state on top of which the collective mode is built has already suggested the use of *GDR* properties in order to study nuclei far from the ground state. The time structure of the *GDR* mode actually allows a possibility of using it as a probe of nuclear systems very far from normal conditions, see the nice reviews [2,3].

We can roughly estimate an oscillation period of $\frac{2\pi\hbar}{E_{GDR}} \simeq 80 - 100 \text{ fm}/c$ and a mean life-time $\hbar/\Gamma_{GDR} \simeq 50 \text{ fm}/c$. Since the spreading width is the largest contribution to the total width Γ_{GDR} , $50 \text{ fm}/c$ is roughly also the time needed to build up the collective *GDR* mode in a Compound Nucleus (C.N.). All these time scales are relatively short and this makes the *GDR* an ideal probe to study nuclear systems under extreme conditions.

Charge equilibration takes place on time scales of few units in $10^2 \text{ fm}/c$: therefore in charge asymmetric entrance channels we expect to see a "direct dipole" collective excitation, with special dynamical features, which should give an extra yield to the photon spectrum in the *GDR* region. The idea is that we can form a fused dinuclear system with the charge not yet equilibrated and therefore with some extra dipole strength of non statistical nature. In this sense the "*Dynamical Dipole*" is a direct dipole contribution present in dissipative collisions initiated in charge asymmetric entrance channels. This new pre-equilibrium collective mode has been predicted some years ago [4,5] and recently clearly observed in fusion [6–8] and deep-inelastic [9,10] reactions. Some experiments have been performed also at intermediate energies, where other dynamical entrance channel features can be present [11,12]. The appearance of this prompt dipole effect gives important information on the charge equilibration dynamics in connection to the reaction mechanism. A fully microscopic analysis is performed with quantitative predictions of the *GDR* photon yield based on a dynamics-statistics coupling model. Independent information on the damping of the dipole mode in very excited nuclear systems can be derived. Moreover the coupling between isovector dipole

and large amplitude isoscalar monopole oscillations can be studied, of large interest also for the discussion on the fate of the *GDR* in hot nuclei. Since the effect is strongly dependent on fusion dynamics we study the beam energy variation of this extra dipole strength and we suggest some optimal conditions for the relative observation.

II. GDR IN CHARGE ASYMMETRIC FUSION: THE DYNAMICAL DIPOLE

Fusion processes in charge asymmetric entrance channels give a clear example on how emitted *GDR* photons carry information on a Compound Nucleus (*CN*), formed during the reaction dynamics, very far from normal conditions.

In dissipative collisions energy and angular momentum are quickly distributed among all single particle degrees of freedom while charge equilibration takes place on larger time scales [13]. Therefore for charge asymmetric entrance channels at the time of *CN* formation we can easily have some relic of a pre-equilibrium *GDR* from dipole oscillations in the isospin transfer dynamics [5]. The result will be an enhanced *GDR* photon emission with special features due to the non-statistical nature of this extra contribution.

An enhancement of the *GDR* gamma ray yield has been observed experimentally in fusion reaction between heavy ions with different neutron to proton ratios. Flibotte et al. [6], in collision between ^{40}Ca ($N/Z = 1$) and ^{100}Mo , ($N/Z = 1.38$), at $4AMeV$ beam energy, producing a *CN* at $70MeV$ excitation energy, counted a number of emitted *GDR* photons over the whole cascade 16% larger than in the case when the same *CN* was formed with a symmetric N/Z combination. Similar effect has been observed by Cinausero et al. [7]: an increase of 36% resulted when they compared *GDR* photon yields from a *CN* populated at 110 MeV excitation energy via the reactions ^{16}O ($N/Z = 1$) + ^{98}Mo ($N/Z = 1.33$) and ^{50}Ti ($N/Z = 1.18$) + ^{64}Ni ($N/Z = 1.28$) respectively.

In fact, theoretically, an extra-yield of gamma rays was predicted some years ago by Chomaz et al., [5], in a simple model of a *GDR* phonon gas interacting with the *CN*. The essential quantity in this approach is the mean number of excited *GDR* phonons at the time

when a CN is formed, $n_{GDR}^{(0)}$. The emission of GDR photons is enhanced if $n_{GDR}^{(0)}$ is greater than the value corresponding to a statistical equilibrium between the GDR oscillator and the CN heat bath. The N/Z asymmetry of colliding heavy ions will certainly trigger in the early stage of the reaction the charge equilibration process. Several experiments and realistic simulations have indicated that the related dipole oscillation has the characteristics of a GDR type quantal collective motion [13], [14], [15], [16], [17], [18]. Expressed in terms of the Brink-Axel hypothesis [19] this means that a GDR may be built not only on equilibrium states, of a warm nucleus for example, but also on non-equilibrium states during the CN formation phase. $n_{GDR}^{(0)}$ represents just the number of phonons in this mode at the time of the CN formation, t_{CN} .

Although it was assumed that the quantity $n_{GDR}^{(0)}$ is intimately related to the presence of pre-equilibrium effects, the way it is determined and affected by the projectile-target N/Z asymmetry and entrance-channel dynamics has not been investigated yet. From the previous discussion we clearly distinguish three main phases in the entrance channel dynamics: *I - The approaching phase*, with the two partners still keeping their own response properties; *II - The dinuclear phase*, with relative collective response; *III- The CN formation*. We will call $t = 0$ the starting time of the phase *II*, i.e. the onset of the main dissipation mechanisms, including the charge equilibration. In this phase a pre-equilibrium dipole mode is present in the composite system, damped with a spreading width $\Gamma^\downarrow \equiv \hbar\mu(t)$, where the time dependence is expressing a non-equilibrium situation. The correspondent number of phonons will show an exponential decrease:

$$n(t) = n_i e^{-\int_0^t \mu(t) dt} \quad (1)$$

where n_i is the number of phonons at the moment when charge equilibration begins. Fusion experiments seem to indicate that this will happen once the decision for fusion is taken [13]. This means that when the system passes from the strong absorption configuration through the barrier the neck is large enough to allow for an isospin collective motion. Therefore we can assume that the configuration reached soon after, when the interdistance between the

center of mass of the two nuclei is around the sum of their radii, represents the starting point of the collective pre-equilibrium *GDR* mode. It is important to stress that at this moment we have already reached a quite noticeable density overlap and therefore the considered configuration is not corresponding to the naive picture of the two nuclei as two touching rigid spheres. This will become clear from density contour plots and collective behaviours we will show later in microscopic dynamical simulations.

In order to estimate n_i we consider a harmonic oscillator description for the *GDR*:

$$H_{GDR}(t) = \frac{\Pi^2(t)}{2M} + \frac{M\omega^2(t)}{2}X^2(t), \quad (2)$$

where $M = \frac{ZN}{(Z+N)}m$ is the reduced mass of the neutron-proton relative motion, $m = 935\text{MeV}$ being the nucleon mass, $N = N_1 + N_2$, ($Z = Z_1 + Z_2$), the total number of neutrons (protons).

Here Π denotes the relative momentum:

$$\Pi = \frac{NZ}{A} \left(\frac{P_p}{Z} - \frac{P_n}{N} \right) \quad (3)$$

with P_p (P_n) the center of mass momentum for protons (neutrons), while $X = R_p - R_n$ is the distance between the centers of mass of the two components. The initial number of phonons is defined as:

$$n_i = \frac{H_{GDR}(0)}{\hbar\omega(0)} \approx \frac{1}{2\hbar^2} M(\hbar\omega(0)) X^2(0) \quad (4)$$

We use the above approximation in order to get a closed form directly related to the initial charge asymmetry since $X(0)$ is given by:

$$X(0) = \frac{Z_1 Z_2}{NZ} \left(\frac{N_1}{Z_1} - \frac{N_2}{Z_2} \right) (R_1 + R_2) \quad (5)$$

In Eq.(4) we are neglecting the kinetic part contribution. We expect this approximation not to work at higher incident beam energies. This contribution will be thoroughly accounted for from dynamical simulations, as discussed later.

We can consider for the initial elongated shape a phonon energy [20]:

$$\hbar\omega(0) = \frac{R}{R_1 + R_2} E_{GDR} \quad (6)$$

where $R = r_0 A^{1/3}$, ($r_0 = 1.2$), is the equilibrium radius of the CN and $E_{GDR} \simeq 78A^{-1/3}$ is the energy of a phonon built on CN , corresponding to the centroid of the GDR spectrum in medium-heavy nuclei.

In conclusion we can finally express the mean number of phonons at the time when a CN is formed as:

$$\begin{aligned} n_{GDR}^{(0)} = n(t_{CN}) &\approx \frac{1}{2\hbar^2} MR(R_1 + R_2) \frac{Z_1^2 Z_2^2}{N^2 Z^2} \left(\frac{N_1}{Z_1} - \frac{N_2}{Z_2} \right)^2 E_{GDR} \exp(-\mu_{ave} t_{CN}) \\ &= 1.4 \frac{(A_1^{1/3} + A_2^{1/3})}{A} \frac{Z_1^2 Z_2^2}{NZ} \left(\frac{N_1}{Z_1} - \frac{N_2}{Z_2} \right)^2 \exp(-\mu_{ave} t_{CN}) \end{aligned} \quad (7)$$

where μ_{ave} is an average value of the spreading width:

$$\mu_{ave} = \frac{1}{t_{CN}} \int_0^{t_{CN}} \mu(t) dt \quad (8)$$

We observe that $n_{GDR}^{(0)}$ will depend critically on fusion dynamics (through the time scale for Compound Nucleus formation) as well as on properties of the spreading width $\mu(t)$.

After the time t_{CN} we have to switch to the approach introduced in [5] for the CN decay phase. The number of GDR phonons is still time-dependent since charge equilibration is still going on, but now we can have some feeding from the CN heat bath with a width $\Gamma_{feed} \equiv \hbar\lambda$. The result is [5] (now the origin of time is t_{CN}):

$$n_{GDR}(t) = \frac{\lambda}{\mu} \left[1 - (1 - n_{GDR}^{(0)} \frac{\mu}{\lambda}) \exp(-\mu t) \right] \quad (9)$$

which asymptotically leads to the statistical value:

$$\frac{\lambda}{\mu} = \frac{\rho(E^* - E_{GDR})}{\rho(E^*)} \approx \exp(-E_{GDR}/T), \quad (10)$$

where $\rho(E)$ is the level density, E^* is the CN excitation energy and T the corresponding temperature. From this discussion we see that the quantity Eq.(9) can be directly used as the dipole strength in the evaluation of γ -decay in the CN evaporation cascade. From the detailed balance we have a statistical γ emission rate:

$$R_\gamma(E_\gamma) = \frac{\rho(E^* - E_\gamma)}{\rho(E^*)} \frac{\sigma_{abs}(E_\gamma)}{3} \frac{E_\gamma^2}{(\pi\hbar c)^2} = \frac{\rho(E^* - E_{GDR})}{\rho(E^*)} \left[\frac{\rho(E^* - E_\gamma)}{\rho(E^* - E_{GDR})} \frac{\sigma_{abs}(E_\gamma)}{3} \frac{E_\gamma^2}{(\pi\hbar c)^2} \right] \quad (11)$$

where $\sigma_{abs}(E_\gamma)$ is the absorption γ -dipole cross section. This leads, in presence of a pre-equilibrium contribution, to a time dependent quantity:

$$R_\gamma(E_\gamma, t) = n_{GDR}(t) \left[\frac{\rho(E^* - E_\gamma)}{\rho(E^* - E_{GDR})} \frac{\sigma_{abs}(E_\gamma)}{3} \frac{E_\gamma^2}{(\pi \hbar c)^2} \right] \quad (12)$$

with $n_{GDR}(t)$ given by Eq.(9).

The final yield of photons emitted can be then evaluated using a time-dependent evaporation cascade procedure, see ref. [21]. From Eq.s(12) and (9), once the CN initial excitation energy (temperature) is fixed, the results will be critically dependent on $n_{GDR}^{(0)}$ and $\Gamma^\downarrow(T)$.

To show how the method is working and the sensitivity to the above parameters in Fig.1 we report some results for the systems studied by Flibotte et al [6]. The curves represent the "subtracted" photon spectra (i.e. normalized to a statistical emission without GDR): in (a) the data for the two systems, $Ca + Mo$ (charge asymmetric, dashed) and $S + Pd$ (more symmetric, solid), and in (b), (c), (d) the results obtained from 10^5 runs of a Monte Carlo evaporation cascade [22,21] with the same initial conditions for the CN and varying only $n_{GDR}^{(0)}$ and $\Gamma^\downarrow(T)$. The best results (Fig.1b) are obtained with the values $n_{GDR}^{(0)} = 0.14$ and $\Gamma^\downarrow = 8 MeV$. Now while it is reasonable to have a GDR damping width larger than in the ground state of the same compound nucleus ^{140}Sm ($\Gamma^\downarrow = 4.8 MeV$ used in Fig.1c) the choice of $n_{GDR}^{(0)}$ requires a deeper dynamical justification. This will be discussed later in a detailed connection to the fusion dynamics that will allow some interesting predictions on the beam energy dependence of this GDR extra strength.

III. DYNAMICAL DIPOLE SIGNATURE ON ANGULAR DISTRIBUTIONS

We note that the pre-equilibrium contribution has some special dynamical features, being associated with a dipole component on the reaction plane, actually along the symmetry axis of the dinuclear system. If we call this as the z -component, we expect no dipole strength present on the x, y components at the time of the CN formation. The corresponding number of phonons will also reach asymptotically the statistical value Eq.(10) (times 1/3 on average) but starting from zero at $t = t_{CN}$ [23].

We have then time dependent γ -dipole emission rates different for each component in the intrinsic reference system of the dinucleus:

$$\begin{aligned} R_{\gamma,z}(E_\gamma, t) &= \left[\frac{\lambda}{3\mu} (1 - \exp(-\mu t)) + n_{GDR}^{(0)} \exp(-\mu t) \right] \frac{\sigma_{abs}(E_\gamma)}{3} \frac{E_\gamma^2}{(\pi\hbar c)^2} \\ &\equiv W_z(t) \frac{\sigma_{abs}(E_\gamma)}{3} \frac{E_\gamma^2}{(\pi\hbar c)^2} \end{aligned} \quad (13)$$

$$\begin{aligned} R_{\gamma,x}(E_\gamma, t) = R_{\gamma,y}(E_\gamma, t) &= \left[\frac{\lambda}{3\mu} (1 - \exp(-\mu t)) \right] \frac{\sigma_{abs}(E_\gamma)}{3} \frac{E_\gamma^2}{(\pi\hbar c)^2} \\ &\equiv W_{x,y}(t) \frac{\sigma_{abs}(E_\gamma)}{3} \frac{E_\gamma^2}{(\pi\hbar c)^2} \end{aligned} \quad (14)$$

with $n_{GDR}^{(0)}$ given by Eq.(7).

We remark the physical meaning of the time dependent weights $W_{z,x,y}(t)$ defined before, they represent the number of dipole phonons on each component at each time step. In Fig.2 we report a typical behaviour of the weights. We have chosen the parameters corresponding to the $Ca + Mo$ system of ref. [6], see before.

In particular we note the extreme values at $t = 0$ (CN formation time) and asymptotically $t \rightarrow \infty$ (full charge equilibration):

$$W_z(0) = n_{GDR}^{(0)} \quad , \quad W_z(\infty) = \frac{\lambda}{3\mu} \quad (15)$$

$$W_{x,y}(0) = 0 \quad , \quad W_{x,y}(\infty) = \frac{\lambda}{3\mu}, \quad (16)$$

i.e. the GDR phonons are initially only on the z -component and finally uniformly distributed on the three axes. This property will have important observable effects on the γ -angular distributions.

The angular distribution of the emitted photons can be written as [24,3,25,26] :

$$W(\theta, E_\gamma) = W_0(1 + a_2(E_\gamma)P_2(\theta)) \quad (17)$$

where $P_2(\theta)$ is a Legendre Polynomial in the polar angle θ between the direction of the emitted γ -ray and the beam axis. With our choice of the oscillation axes we have

(x, z) -stretched and y -unstretched transitions [24] and a time-dependent anisotropy parameter:

$$a_2(E_\gamma, t) = \frac{W_y/2 - (W_z + W_x)/4}{W_x + W_y + W_z}, \quad (18)$$

with the time dependent weights $W_{z,x,y}(t)$ given by Eq.s (13,14). The z - extra strength contribution should therefore lead to clear negative values around the *GDR* energy *also in absence of an intrinsic deformation of the fused nucleus*. We remark that all the previous equations can be easily extended to the use of different Lorentzians for the various axis contributions to σ_{abs} , to take into account the presence of deformations. The dynamical dipole effect will enhance the corresponding characteristic anisotropies in the γ - angular correlations.

IV. THE INTERPLAY BETWEEN FUSION DYNAMICS AND PRE-EQUILIBRIUM GDR

In this section we present a fully microscopic analysis of the fusion reaction for some systems of interest, to look in particular at the pre-equilibrium GDR population. The calculations are performed in the framework of the BNV transport equation which incorporates in a self-consistent way the mean field and two-body collisions dynamics [27]. The numerical accuracy has been largely improved in order to have a good description also of low energy fusion reactions, see discussion in [18,26]. Moreover in order to further reduce numerical fluctuations the results presented here are obtained from an average over several events. For the mean field we have adopted a Skyrme-like parametrization, as described in [18], which well reproduces Nuclear Matter saturation properties (equilibrium density, binding energy, compressibility and symmetry energy). In the collision integral we use in medium reduced nucleon-nucleon cross sections, isospin as well as energy and angular dependent [28].

We have focussed our attention on the fusion reaction induced by ^{16}O ($N/Z = 1$) on ^{98}Mo ($N/Z = 1.33$) (see [7]). We have studied in a relative large range of incident beam energy, at

$4\text{MeV}/n$, $8\text{MeV}/n$, $14\text{MeV}/n$ and $20\text{MeV}/n$, the evolution of the composite system along the fusion path. We will consider results that correspond to an impact parameter $b = 0$ as well representative of the features we are looking for.

As discussed in the previous section an essential point is to evaluate the starting time of phase II , when charge equilibration and the relative collective dipole are present in the dinuclear system. This time can be directly extracted from the collision simulation just comparing the evolution of the distance between Projectile-Target Centers of Mass, $d_{PT}(t)$, and of the distance between Neutron-Proton Centers of Mass, $X(t)$, reported in Fig.3. The two quantities are roughly proportional up to the time of the onset of a collective dipole response of the dinuclear system. At this time step, chosen as $t = 0$ in Fig.3, the quantity $X(t)$ clearly shows an acceleration due to the symmetry term of the dinuclear mean field. We remark that for all energies the value of the d_{PT} distance corresponding to the bending of the "dipole" variable $X(t)$ is very close to the sum of the two radii, in agreement with the discussion of the previous section.

In all the following plots we will choose as $t = 0$ such starting time of the dinuclear dynamics, roughly corresponding to the "touching" configuration.

At each time step we can evaluate the dinuclear dipole moment in coordinate and momentum space:

$$DR(t) = \frac{NZ}{A}X(t) \quad (19)$$

$$DK(t) = \frac{\Pi(t)}{\hbar} \quad (20)$$

The results are shown in Fig.4. The out of phase behaviour of the two dipoles, clear signature of a collective dinuclear response, is indeed starting just after $t = 0$ (touching configuration) practically for all energies. We remark a smaller initial amplitude of the oscillation at the lowest (4AMeV) and highest (20AMeV) energies, as well as an increase of the damping with the beam energy. In conclusion it clearly appears an optimum range of energies for the observation of the dynamical dipole effect, well above the Coulomb threshold (about 4AMeV in the $O + Mo$ system) but also well below the Fermi energy domain. This point

will be further analysed in the following.

Fig.5 shows phase-space trajectories of the *GDR*, i.e. the time evolution of the $DK-DR$ correlation. The spiral curves are nicely revealing an out of phase behaviour in presence of some damping. The spiralling trend is starting at the touching configuration ($t = 0$, left points of the curves), maybe with some delay in the lowest energy case. The centre is reached when charge equilibration is achieved. From this time onwards the *GDR* mode will be only of statistical nature. The spiral shows a faster collapse to the central region at high beam energy (Fig.5d) since we have a larger damping of the dynamical collective motion, as already seen in Fig.4.

The amplitude reduction at $4AMeV$ and $20AMeV$ is also evident: the nature of the effect is however different in the two cases. At low energy, just above the Coulomb barrier, the neck is formed quite slowly (see Fig.6) and so the collective dipole response of the dinuclear system is actually starting sometime after the touching configuration, when some charge equilibration has already taken place. At $20AMeV$ the fusion dynamics is fast but now we can have some prompt particle emission that will reduce the dipole moment of the dinucleus. Just by chance we see a quite good spiralling behaviour at $8AMeV$, where the experiment has been performed by Cinausero et al. [7] with a very clear evidence of the dynamical dipole enhancement.

Now we can dynamically evaluate the number of pre-equilibrium *GDR* phonons $n_{GDR}^{(0)}$ present at the time of the *CN* formation: as shown in the previous section this quantity is essentially ruling the extra emission of *GDR* γ -rays. At each time step the average number of phonons $n(t)$ can be determined from the simulations just dividing the total oscillator energy, as defined by Eq.(2), by the one phonon energy at that instant, $\hbar\omega(t)$, i.e. corresponding to the deformation at the time t . The results are presented in Fig.7. The arrows show the initial value $n(0)$ predicted from Eq.(4), i.e. without dynamical effects. The dashed curve in all four pictures is the analytical expectation of Eq.(1) using a constant spreading width value, $\Gamma^\downarrow = 5MeV$. We remark a quite good overall agreement at low beam energies 4 and $8MeV/n$, (a) and (b). With increasing energy we clearly see in the number

of phonons obtained from the simulations a faster damping which quickly compensates the higher starting point. This is particularly evident at $20\text{MeV}/n$ (Fig.7d) where we have to consider a quite larger value for the spreading width joint to a sizeable kinetic term contribution to the initial number of phonons $n(t = 0)$.

This time evolution of the number of dipole phonons in the dinuclear system will strongly influence the quantity we are looking for, $n_{GDR}^{(0)}$, given by the value of $n(t)$ at the time of Compound Nucleus formation t_{CN} , Eq.(7), the latter being fixed from equilibrium conditions in coordinate and momentum space. In Fig.8 we plot the time evolution of the mass quadrupole moment in \vec{r} -space at the four incident energies. Generally we remark two distinct behaviours in the evolution: a faster decay until the first minimum is reached, followed by a smoother trend accompanied by small oscillations. During the first stage the conversion of relative motion into heat takes place and therefore, in the limits of some more time needed for a final thermal equilibration, the moment when the first minimum is attained will provide us the Compound Nucleus formation time. Our evaluation is in agreement with the information obtained by looking at the quadrupole in \vec{p} -space (see Fig.9), which is a good probe of the energy relaxation time. We can extract t_{CN} values of $120\text{ fm}/c$ at 4AMeV , $80\text{ fm}/c$ at 8AMeV , and around $50\text{ fm}/c$ at the higher energies 14AMeV and 20AMeV . From Fig.7 we get the corresponding $n_{GDR}^{(0)} = n(t_{CN})$ parameters: 0.01 at 4AMeV going up to 0.07 at 8AMeV and finally reducing again down to 0.05 at 14AMeV and to 0.04 at 20AMeV .

To test the correctness of our procedure we have performed a complete evaporation cascade calculation using the above extra dipole strength for the system $O + Mo$ at 8AMeV . The "subtracted" spectra (see definition in section II) are shown in Fig.10, from $2 * 10^5$ Montecarlo events, compared with experimental data from ref. [7]. The agreement is quite good.

Since the time scale of fusion dynamics is playing an important role on the amount of extra dipole strength present at the time of CN formation we expect to see some dependence of the effect also on the mass symmetry in the entrance channel, which is strongly affecting

the fusion time, see [21] and ref.s therein. In order to check this point we have studied the system ^{50}Cr ($N/Z = 1.08$) + ^{64}Ni ($N/Z = 1.28$) with almost the same charge asymmetry of $O + Mo$ but much more symmetric in mass. We have considered central collisions at the beam energies 3.5 and 5.5 AMeV corresponding to the same c.m energies above the coulomb barrier of the first two cases of the $O + Mo$ system. The relative fusion paths are shown in Fig.11 for $100fm/c$ starting from the touching configuration, to be compared with the equivalent Fig.6 of the $O + Mo$. At both energies it is quite evident the longer shape equilibration time. In Fig.12a,b (to compare with Fig.3a,b for $O + Mo$) we see how the dinuclear formation time ($t = 0$ in our convention) can be again well deduced from the simulations. In Fig.12c,d we show the time evolution of the correlation between momentum and space dipoles. If we compare with the analogous Fig.5a,b of the mass asymmetric $O + Mo$ case we clearly observe a quite larger damping of the collective dipole mode in the dinucleus, due to the larger excitation energy available in the more symmetric system and the related increase of the GDR spreading width [26,31]. The slower shape equilibration is quantitatively analysed in Fig.13a,b (see the corresponding Fig.8a,b for $O + Mo$) and finally the time evolution of the number of dipole phonons is presented in Fig.13c,d, to compare with the equivalent Fig.7a,b for the mass asymmetric case. We remark that in spite of the larger initial value $n(t = 0)$, as expected from Eq.(4) since $R_1 + R_2$ is larger in case of mass symmetry, we finally get a much smaller value of $n_{GDR}^{(0)} = n(t_{CN})$ for two main reasons, the larger damping and the longer CN formation time.

We have finally checked the method also for the ref. [6] system, $Ca + Mo$ at 4 AMeV, where the best results are obtained with a $n_{GDR}^{(0)} = 0.14$, see Fig.1. In Fig.14 we present the time evolution of the relevant quantities, mass quadrupole moment, dipole moments in \vec{r} - and \vec{p} - space and average number of phonons. With respect to the $O + Mo$ case at the same energy we see a larger initial dipole strength but with a stronger damping and a slower fusion process. We have a $t_{CN} \simeq 120fm/c$ and a corresponding $n_{GDR}^{(0)}$ ranging between 0.12 and 0.15, as needed in the fitting procedure of Fig.1.

V. SUMMARY AND CONCLUSIONS

We have shown that important information on the early stage of the fusion path can be obtained studying charge-asymmetric reactions. In fact, in this case it is possible to reveal a "direct" dipole oscillations (*the dynamical dipole*), related to the charge equilibration dynamics, which leads to some extra *GDR* strength in the statistical decay of the fused system.

The dynamical nature of such pre-equilibrium contribution, i.e. corresponding to dipole oscillations on the reaction plane, is expected to show up in an anisotropic γ -emission, also in absence of deformations in the compound nucleus.

In this work we have investigated how N/Z asymmetry and fusion dynamics are affecting the properties of the pre-equilibrium *GDR* remnants. We have shown the existence of a *GDR* collective mode, during the formation phase of the compound nucleus, i.e. built on nonequilibrium states. This has allowed us to express the mean number of dipole phonons present in the fused nucleus in terms of the initial isospin asymmetry, *CN* formation time and *GDR* spreading width. We can make quite accurate predictions on the optimal choice of the reaction partners, in particular on the interplay between charge and mass asymmetry in the entrance channel.

Particularly interesting is to follow the energy dependence of the effect. We expect to see a *rise and fall* of the dynamical dipole contribution.

At low energies, just above the Coulomb barrier, the effect is strongly reduced for two combined reasons:

- i) A delay in the dinucleus formation (slow neck dynamics) and relative collective response. The pre-equilibrium dipole oscillation of the composite system will have an initial smaller amplitude since some charge equilibration has already taken place.
- ii) A longer Compound Nucleus formation time is decreasing the average number of phonons present in the fused system due to the *GDR* damping.

At higher energies, close to the Fermi energy domain, the effect is again reduced on average for two main reasons:

- i) We have a relevant pre-equilibrium particle emission (i.e. incomplete fusion events) with a direct reduction of the initial charge asymmetry.
- ii) In the fusion processes we have a large excitation energy deposited in the composite system with a related increase of the *GDR* spreading width leading to a fast decrease of the number of dipole phonons.

Mass symmetry in the entrance channel is also strongly affecting the dynamical dipole extra-strength. For the same charge asymmetry and the same incident energy above the Coulomb barrier more mass symmetric systems are expected to show a more reduced pre-equilibrium *GDR* strength for two main reasons, a longer compound nucleus formation time and a larger *GDR* spreading width due to the larger excitation energy that can be reached in the dinuclear configuration. These two effects are clearly compensating the larger value of the dipole moment at the touching time. An increase of the beam energy will not help for the reasons listed above, pre-equilibrium and larger damping of the collective mode. In conclusion mass-symmetric entrance channels are strongly quenching the dynamical dipole effect at all energies.

Moreover a new dynamical feature is appearing at beam energies above $20AMeV$, some large monopole oscillations in the entrance channel dynamics [29–31]. The dynamical dipole strength is reduced and more fragmented, see the simulations in ref. [31], although still present as confirmed from very recent data [11,12]. The study of the dynamical dipole effect in the Fermi energy domain, although experimentally quite difficult, would therefore bring new independent information on the spreading width of hot *GDR* and in particular on the coupling to an expanding collective mode

Finally, for charge asymmetric reactions, the enhanced dipole emission could be an interesting cooling mechanism to favour the fusion of very heavy nuclear systems.

From the interplay between charge and shape equilibration time-scales we can also suggest new experiments to study the dipole propagation in excited nuclei. The use of radioactive beams will enhance the possibility of such observations.

Acknowledgements

We warmly thank D.M.Brink and Ph.Chomaz for many pleasant and enlightning discussions. We are deeply grateful to the TRASMA experimental group of LNS-Catania, in particular to F.Amorini, G.Cardella, M.Papa and S.Tudisco for the availability of their "fresh" data and for a stimulating interface. Two of us (V.B. and N.T.) acknowledge the INFN support for their stay at the Laboratori Nazionali del Sud, Catania. They also deeply thank the LNS staff for the warm atmosphere and the good working conditions.

REFERENCES

- [1] A. Van der Woude, Nucl.Phys. A599 (1996) 393c
- [2] K.A.Snover, Annu.Rev.Nucl.Part.Sci. 36 (1986) 545
- [3] J.J.Gaardhoeje, Annu.Rev.Nucl.Part.Sci. 42 (1992) 483
- [4] Ph. Chomaz in "Proceedings of the 6th Franco-Japanese Colloquium", St. Malo, France, 1992, edited by N. Alamanos, S. Fortier and F. Dykstra, Saclay (1993)
- [5] Ph.Chomaz, M.Di Toro and A.Smerzi, Nucl.Phys. A563 (1993) 509
- [6] S.Flibotte et al., Phys.Rev.Lett. 77 (1996) 1448
- [7] M.Cinausero et al., Nuovo Cimento A111 (1998) 613
- [8] F.Amorini et al., Phys.Rev. C58 (1998) 987
- [9] M.Trotta et al., RIKEN Review 23 (1999) 96.
M.Sandoli et al., Eur.Phys.J. A6 (1999) 275
- [10] M.Papa et al. , Eur.Phys.J. A4 (1999) 69.
- [11] F.Amorini, TRASMA exp., Ph.D.Thesis LNS Catania 1998.
- [12] S.Tudisco, TRASMA exp., Ph.D.Thesis LNS Catania 1999.
- [13] C. Gregoire, in "Proceedings of the Winter College on Fundamental Nuclear Physics", vol. 1, Trieste, Italy, 1984, edited by K. Dietrich, M. Di Toro, H. J. Mang, pp.497-643.
- [14] H. Hofmann et al., Z. Physik A293 (1979) 229.
- [15] P. Bonche, N. Ngo, Phys. Lett. B105 (1981) 17.
- [16] E. Suraud, M. Pi, P. Schuck, Nucl. Phys. A482 (1988) 187c.
- [17] E. Suraud, M. Pi, P. Schuck, Nucl. Phys. A492 (1989) 294.
- [18] V. Baran et al., Nucl. Phys. A600 (1996) 111.

[19] D.M.Brink, D.Phil.Thesis, Oxford 1955.
 P.Axel, Phys.Rev.126 (1962) 671

[20] P.Ring and P.Schuck, *The Nuclear Many-Body Problem*, Springer-Verlag, New York 1980

[21] M. Cabibbo, V. Baran, M. Colonna and M. Di Toro, Nucl. Phys. A637, (1998) 374.

[22] M. Cabibbo, *MONTECASCA Code*, Ph.D. Thesis, Univ. of Catania 1998

[23] D.M.Brink, Nucl.Phys. A519 (1990) 3c

[24] P.Thirolf et al., Nucl.Phys.A482 (1988) 93c

[25] A.Bracco et al., Phys.Rev.Lett. 74 (1995) 3748

[26] V.Baran et al., Nucl.Phys. A599 (1996) 29c,
 V.Baran et al., Progr.Part.Nucl.Phys. 38 (1997) 263

[27] A.Bonasera et al., Phys.Lett. B221 (1989) 233.
 A.Bonasera et al., Phys.Rep. 243 (1994) 1

[28] G.Q. Li and R. Machleidt, Phys. Rev. C48 (1993) 1702; Phys. Rev. C49 (1994) 566;
 G.Q. Li, private communications. Phys. Rev. **C57** 503 (1998)

[29] P.Piattelli et al., Nucl.Phys.A649 (1999) 181c

[30] T.Suomijarvi, RIKEN Symp.on Dynamics in hot nuclei, p.1,1998

[31] M.DiToro et al., Acta Phys.Polonica B30 (1999) 1331-1352

FIGURE CAPTIONS

Fig. 1 Subtracted γ spectra from a ^{140}Sm CN formed at $E^* = 71MeV$ in the charge asymmetric ($Ca + Mo$ - dashed lines) and symmetric ($S + Pd$ - solid lines) entrance channel: a) Experiment [6]; b), c), d), simulations (see text) with $(n_{GDR}^{(0)}, \Gamma^\downarrow)$ respectively equal to $(0.14, 8MeV)$, $(0.6, 8MeV)$, $(0.14, 4.8MeV)$. 10^5 Montecarlo events.

Fig. 2 Time evolution of the number of phonons on the different intrinsic axes for a ^{140}Sm CN formed at $E^* = 71MeV$ in the charge asymmetric $Ca + Mo$ entrance channel. The used parameters are $E_{GDR} = 15MeV$, $T = 2MeV$, $n_{GDR}^{(0)} = 0.14$ and $\Gamma^\downarrow = 8MeV$.

Fig. 3 Time evolution of the distance between Projectile-Target Centers of Mass $d_{PT}(t)$ (solid lines, left scales in fm) and of the distance between Neutron-Proton Centers of Mass $X(t)$ (dashed lines, right scales in fm) for the $O + Mo$ system at beam energies: a) $4AMeV$, b) $8AMeV$, c) $14AMeV$, d) $20AMeV$. The $t = 0$ choice is discussed in the text.

Fig. 4 Time evolution of the dipole moment in \vec{r} -space, DR (solid lines, left scales in fm) and in \vec{p} -space, DK (dashed lines, right scales in fm^{-1}) for the $O + Mo$ reaction. $t = 0$ corresponds to the touching configuration (see text). The labels correspond to the same energies of Fig.3.

Fig. 5 Phase space trajectory of the entrance channel dipole for the $O + Mo$ reaction. The labels correspond to the same energies of Fig.3.

Fig. 6 Density plots of the neck dynamics for the $O + Mo$ system at the two energies $4AMeV$ and $8AMeV$.

Fig. 7 Time evolution of the number of dipole phonons for the $O + Mo$ reaction (solid lines). The labels correspond to the same energies of Fig.3. The dashed line is the reference curve discussed in the text, with a constant spreading width.

Fig. 8 Time evolution of the mass quadrupole moment for the $O + Mo$ reaction (in *a.u.*).

The labels correspond to the same energies of Fig.3.

Fig. 9 Time evolution of the quadrupole moment in momentum space for the $O + Mo$ reaction (in *a.u.*). The labels correspond to the same energies of Fig.3.

Fig. 10 Subtracted γ spectra from a ^{114}Sn *CN* formed at $E^* = 108MeV$ in the charge asymmetric ($O + Mo$ - dashed lines) and symmetric ($Ti + Ni$ - solid lines) entrance channel: a) Experiment [7]; b) simulations (see text) with $(n_{GDR}^{(0)}, \Gamma^\downarrow)$ respectively equal to $(0.07, 7MeV)$. $2 * 10^5$ Montecarlo events.

Fig. 11 Density plots of the neck dynamics for the $Cr + Ni$ system at the two energies $3.5AMeV$ and $5.5AMeV$.

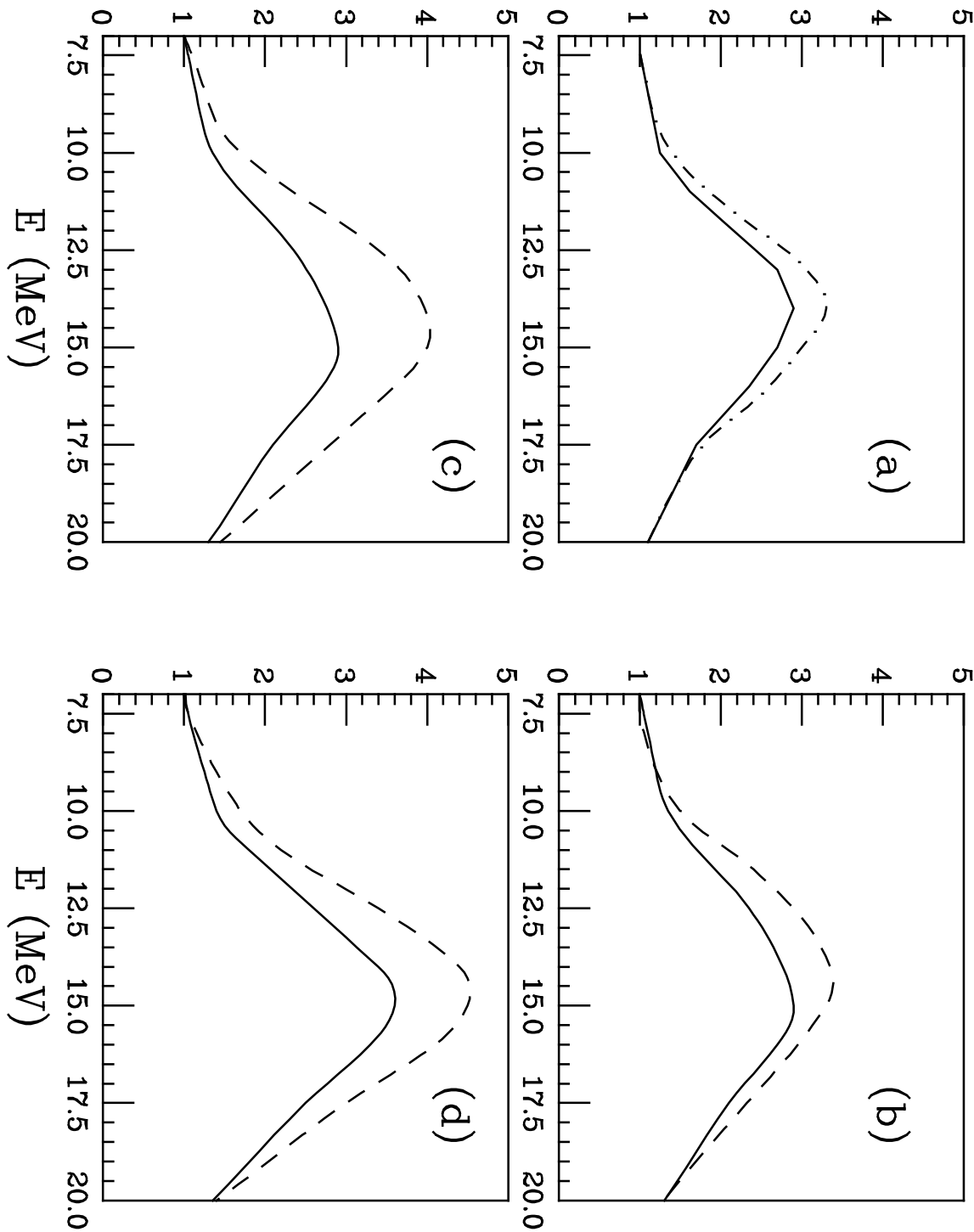
Fig. 12 Collision of the more mass symmetric $Cr + Ni$ system at the two beam energies 3.5 and $5.5AMeV$. (a) and (b): quantities like in Fig.3. (c) and (d): quantities like in Fig.5.

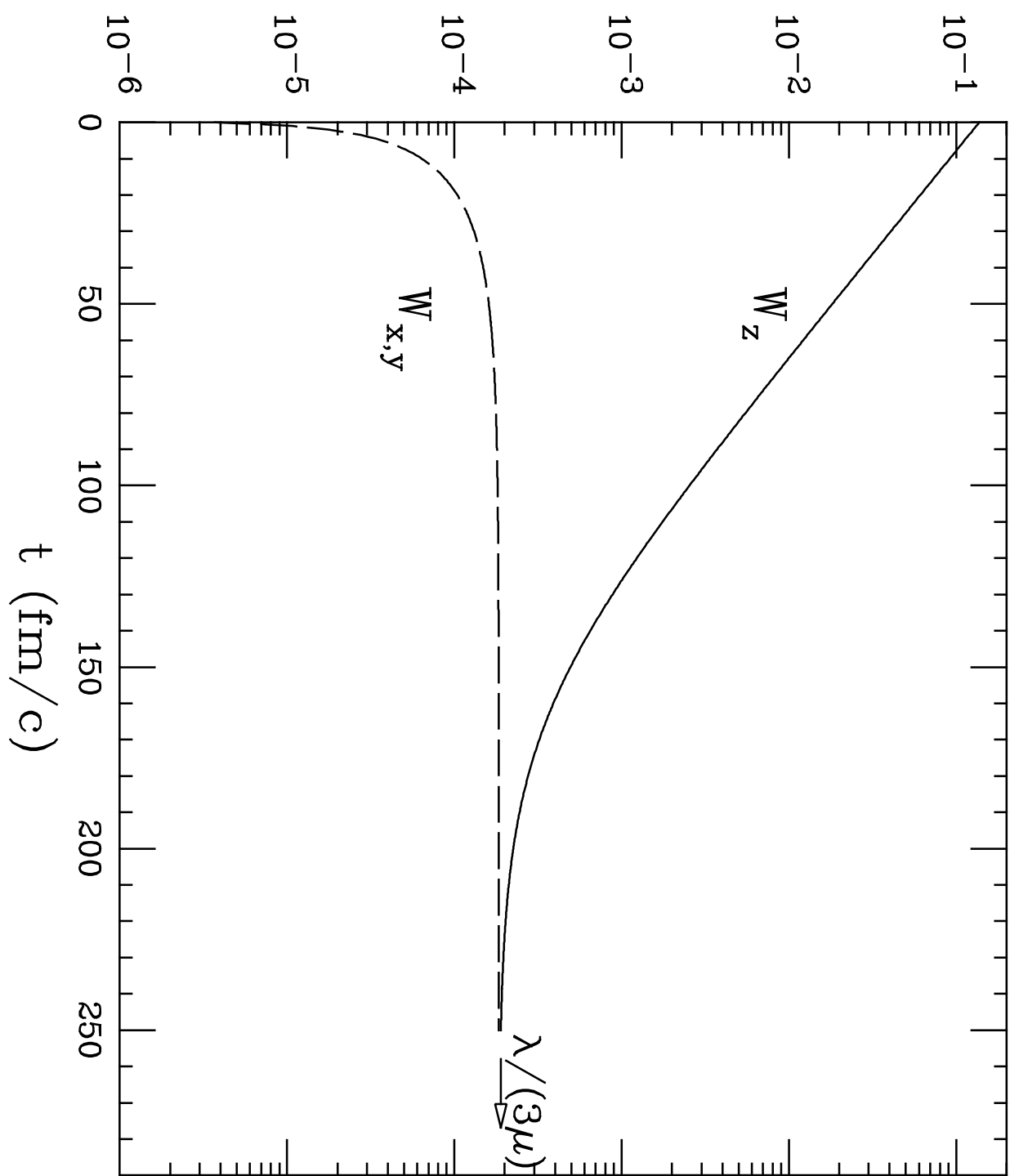
Fig. 13 Collision of the more mass symmetric $Cr + Ni$ system at the two beam energies 3.5 and $5.5AMeV$. (a) and (b): quantities like in Fig.8. (c) and (d): quantities like in Fig.7.

Fig. 14 Time evolution of mass quadrupole moment (a), \vec{r} -dipole moment (b), \vec{p} -dipole moment (c) and average number of dipole phonons (d) for the reaction $Ca + Mo$ at $4AMeV$.

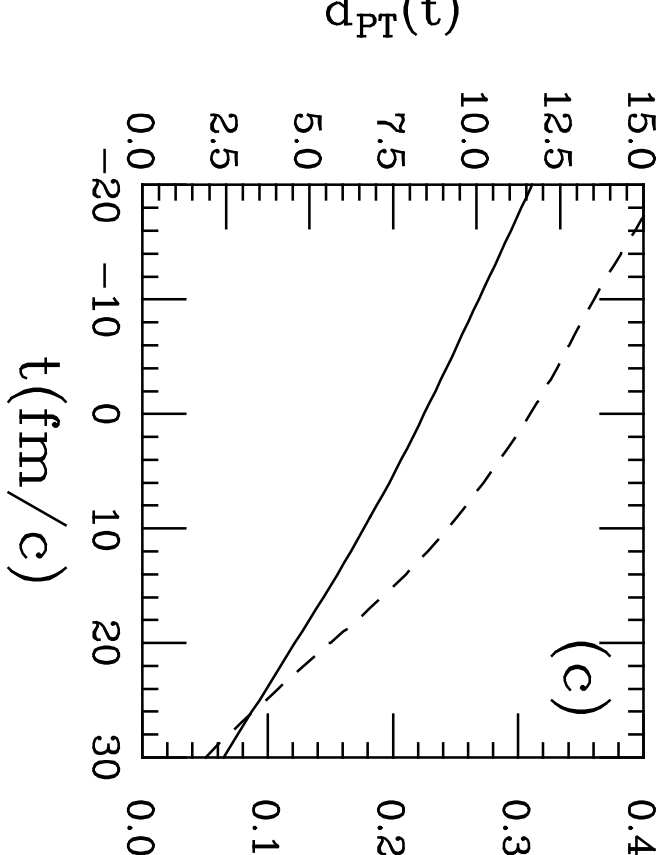
Yields (a.u.)

Yields (a.u.)



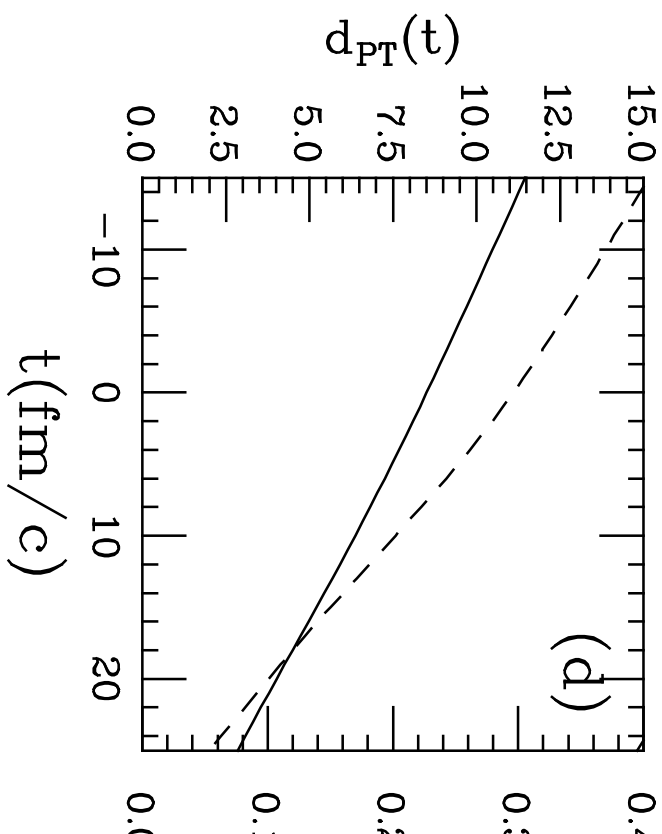


$d_{PT}(t)$



(c)

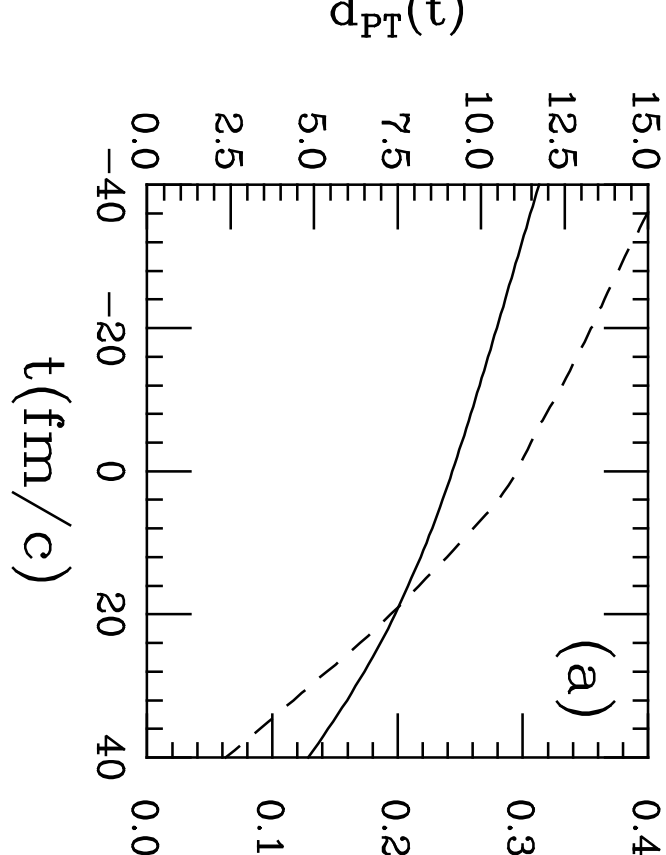
$(\gamma)X$



(d)

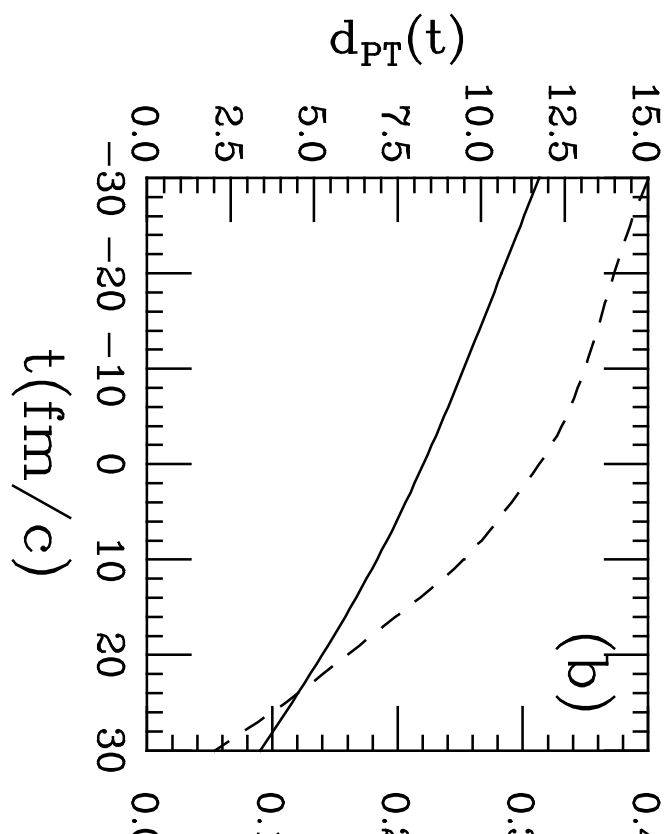
$(\gamma)X$

$d_{PT}(t)$



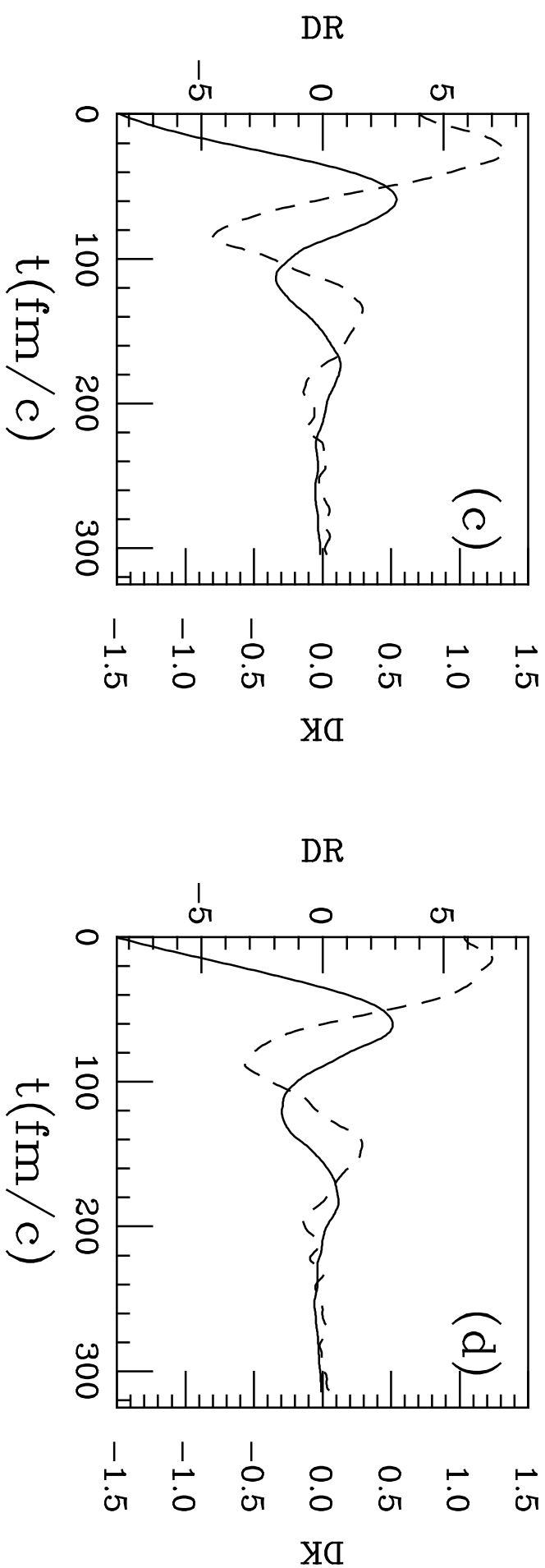
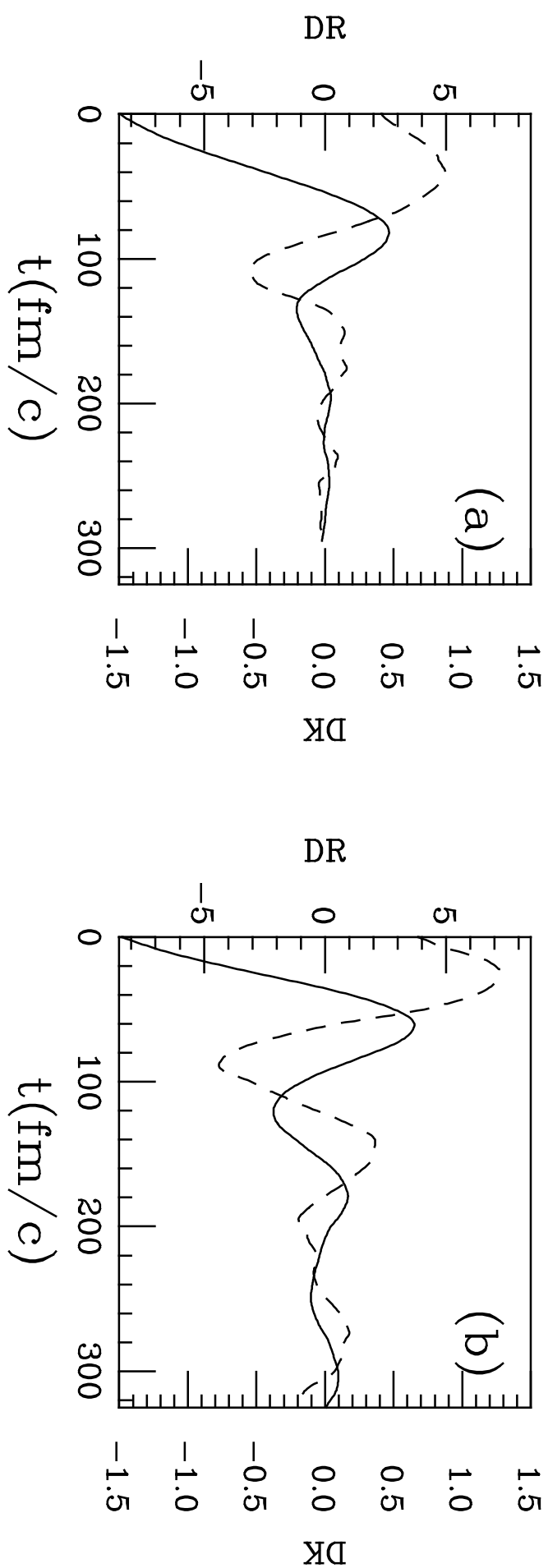
(a)

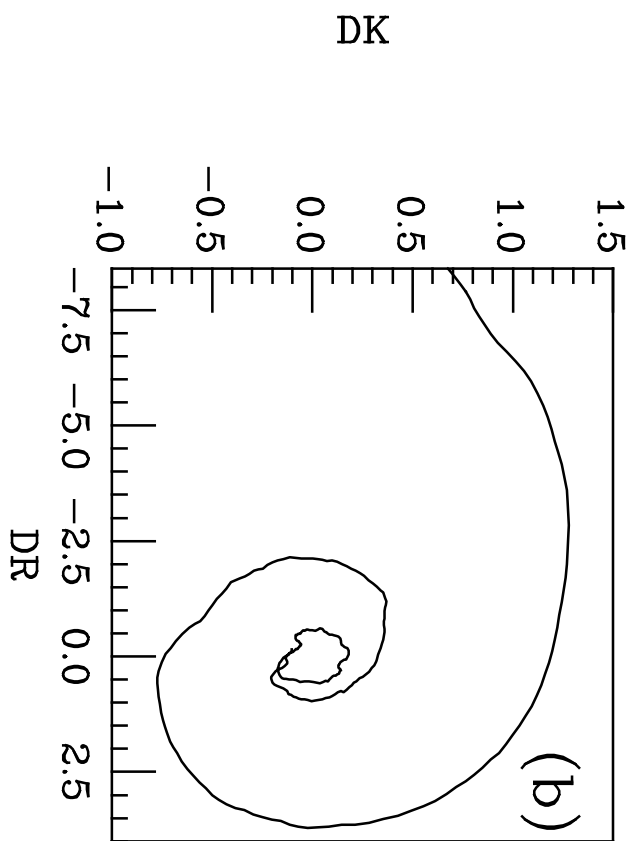
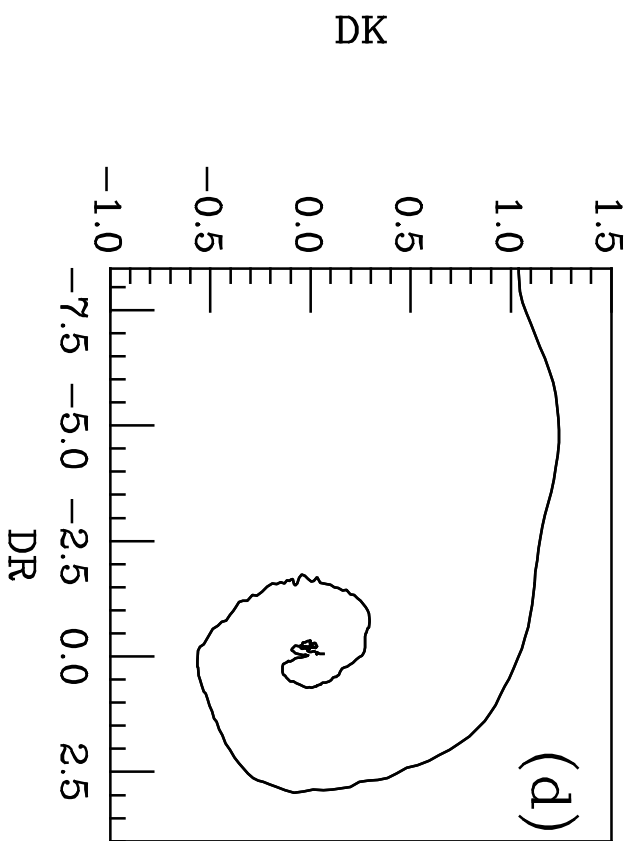
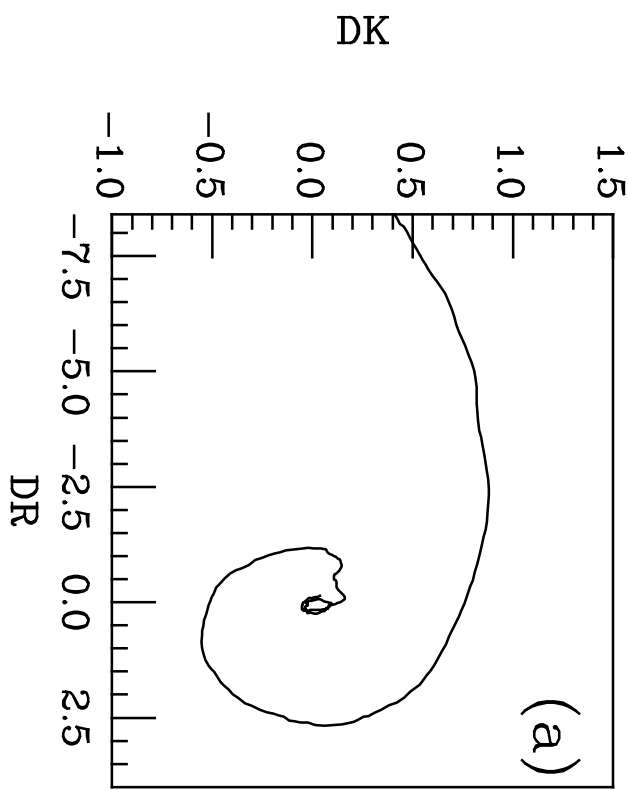
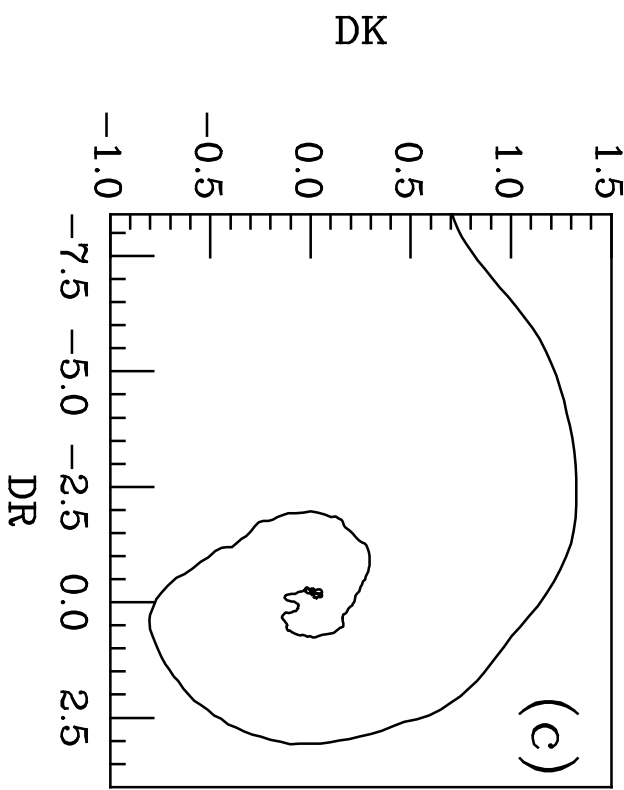
$(\gamma)X$

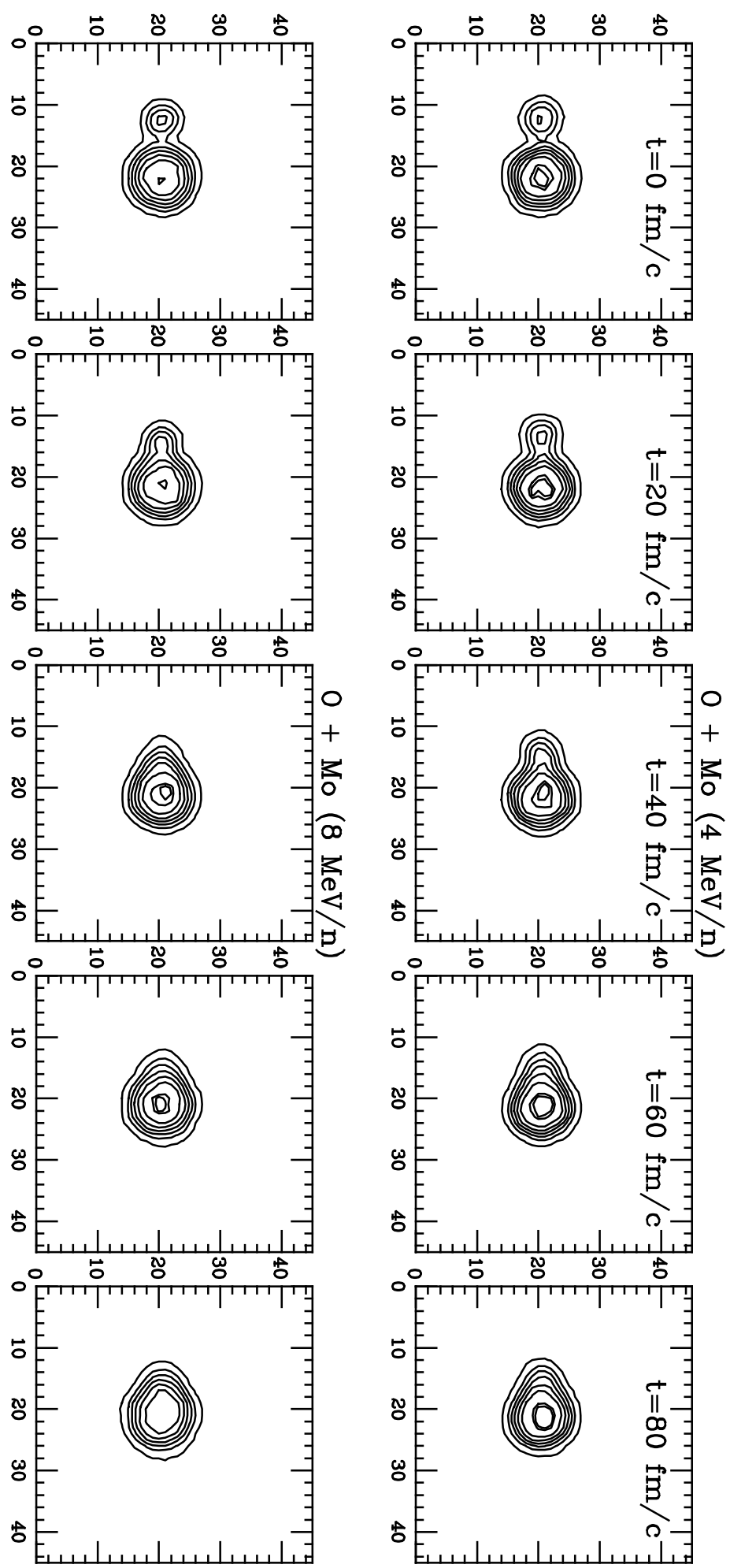


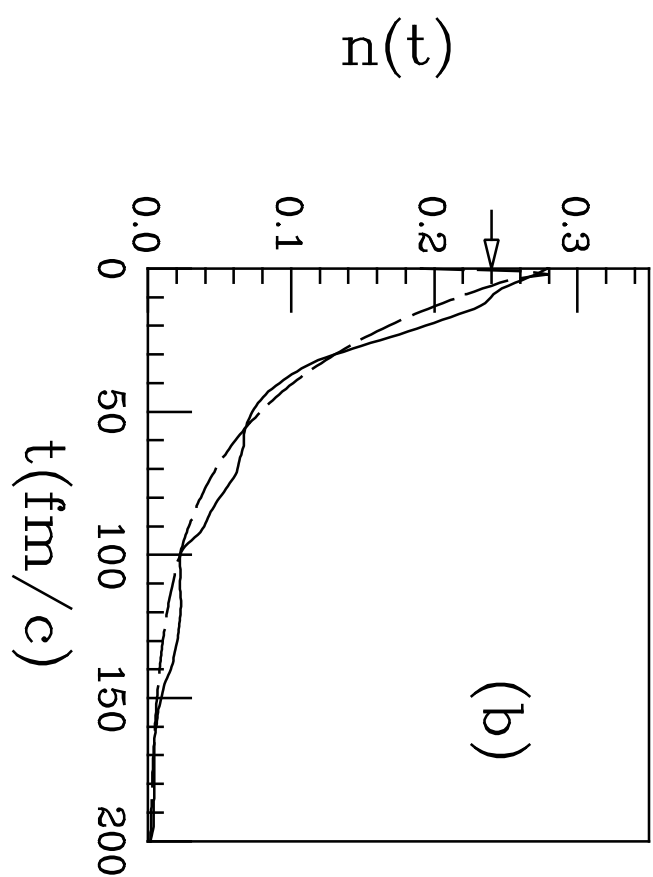
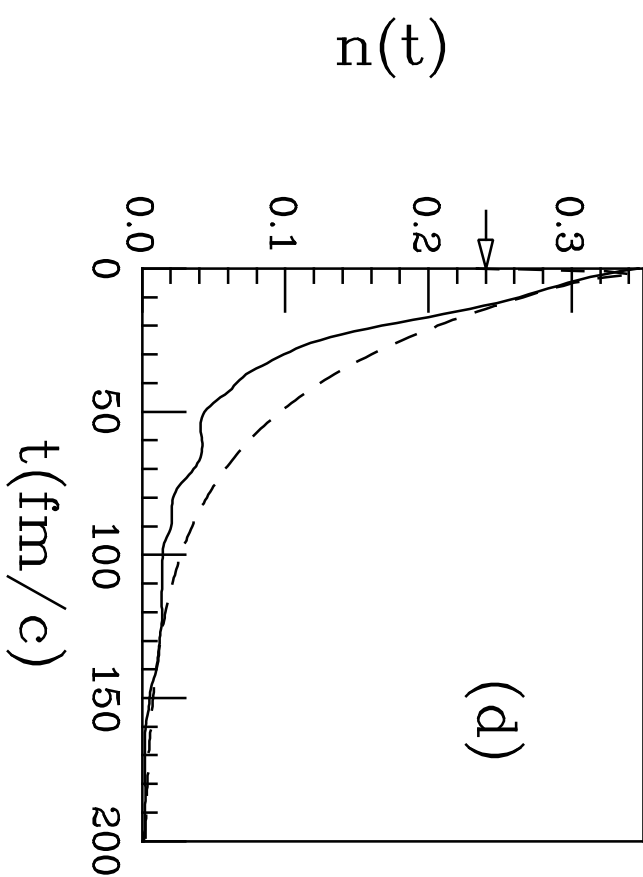
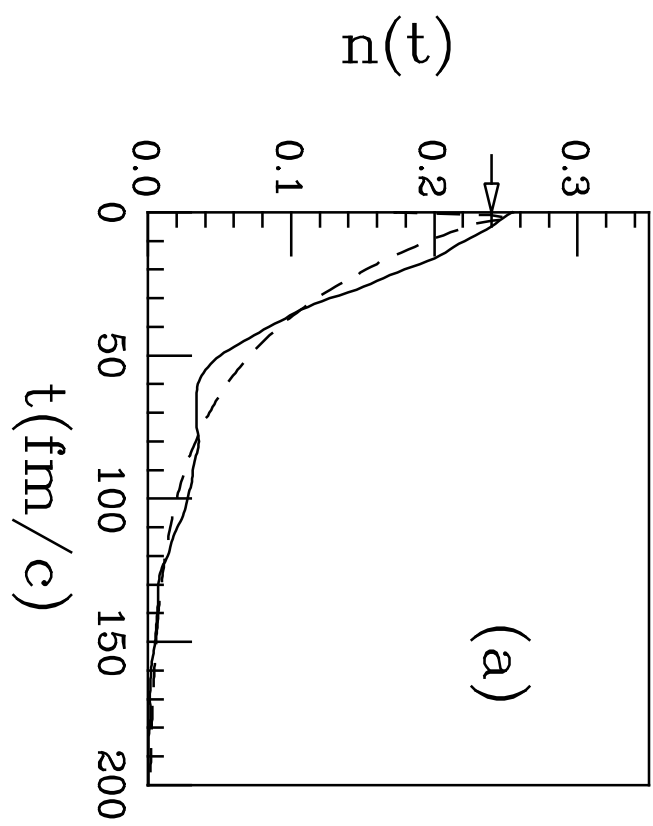
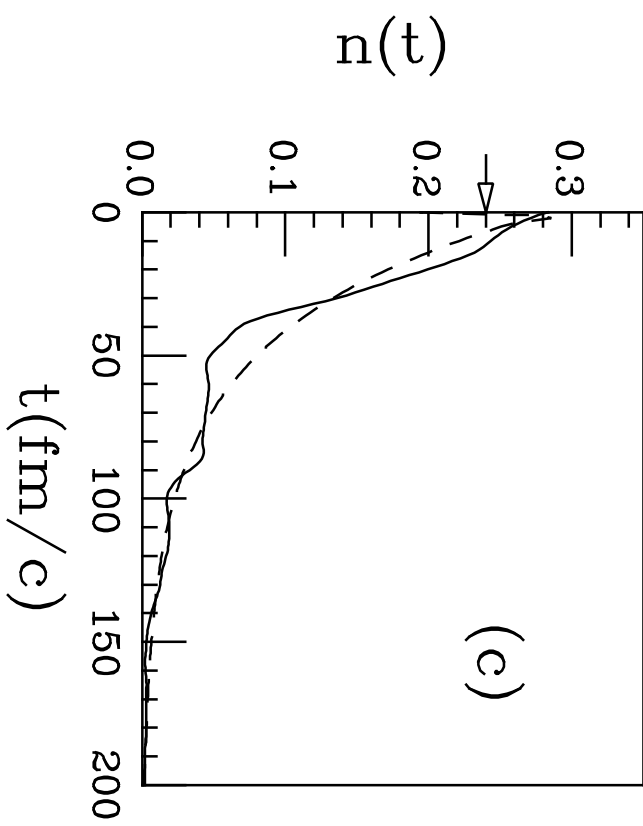
(b)

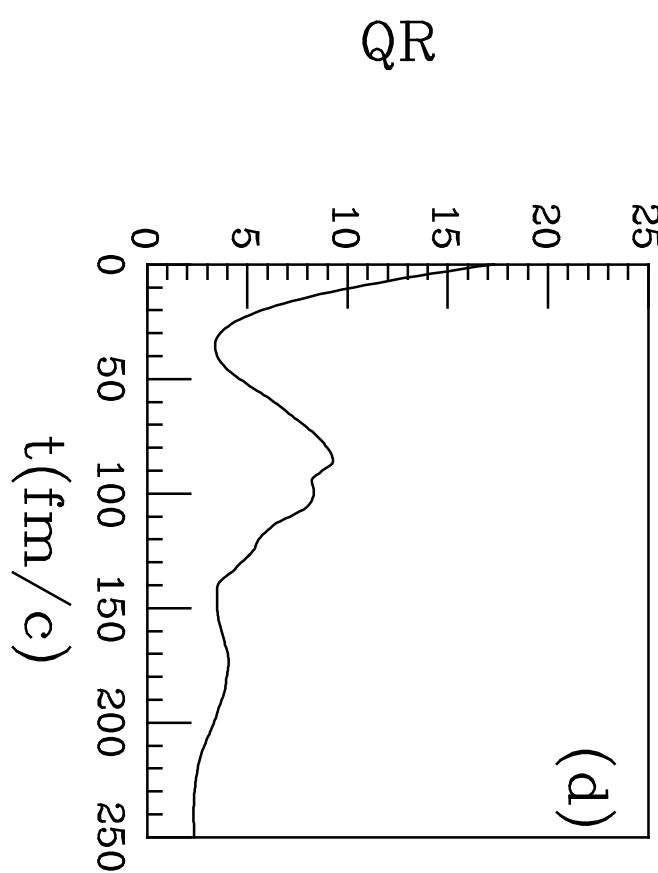
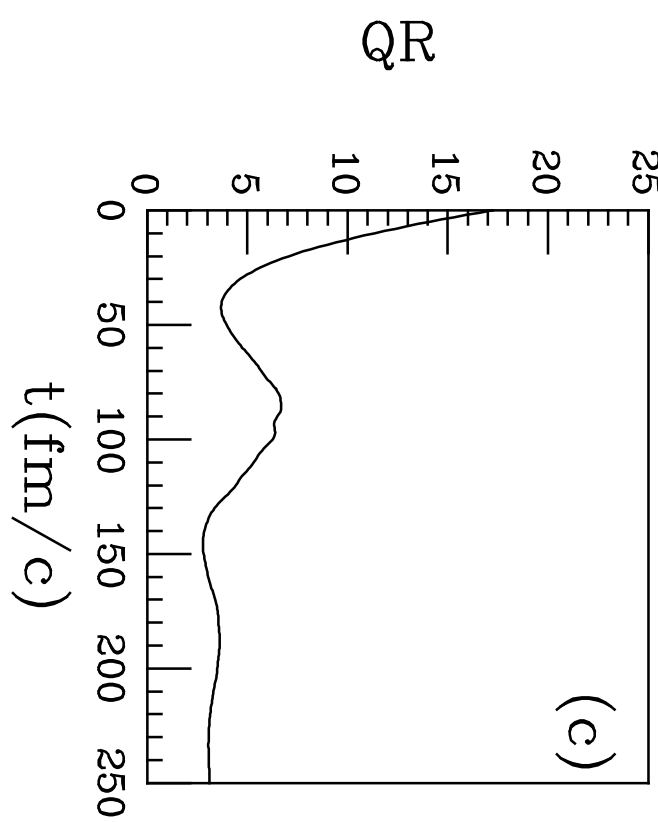
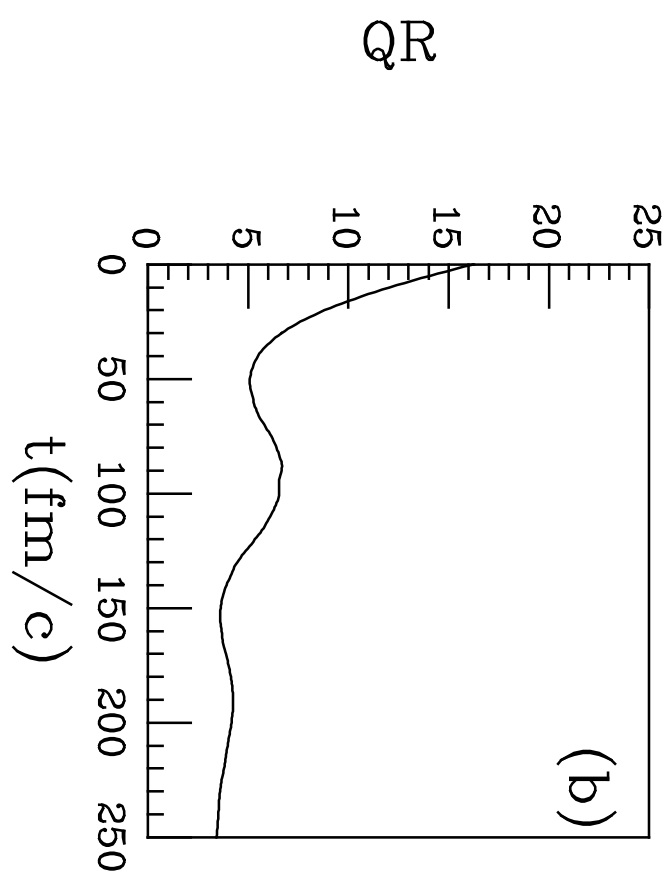
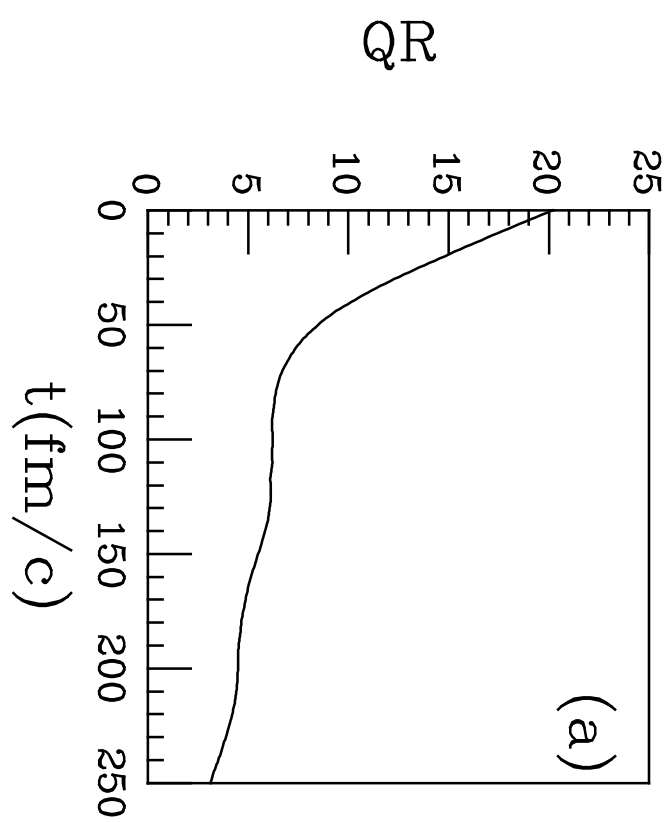
$(\gamma)X$

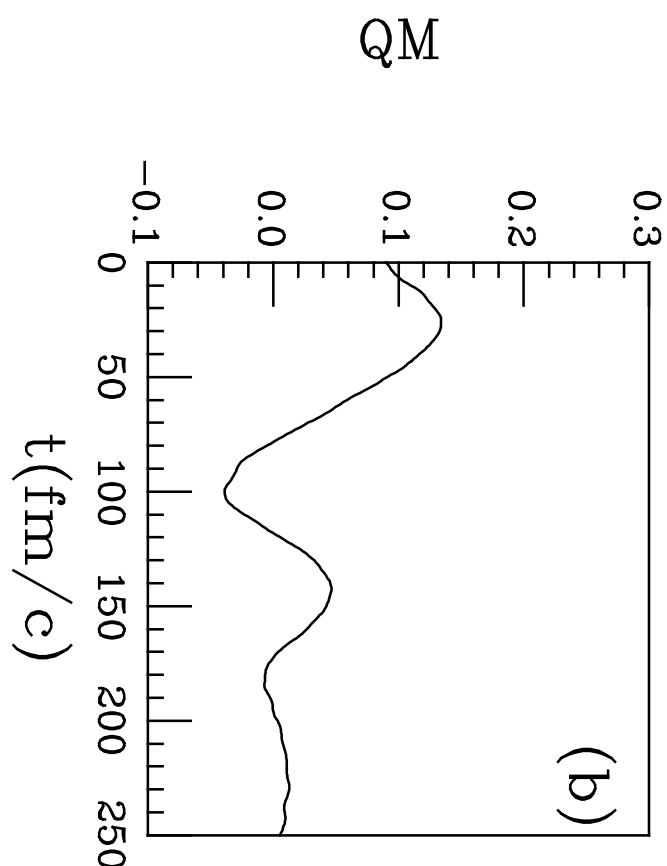
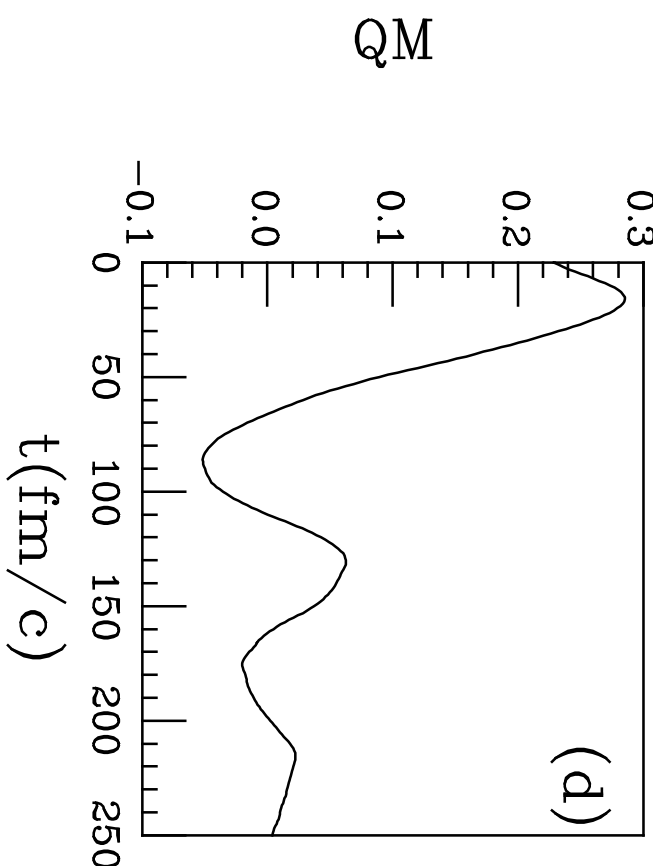
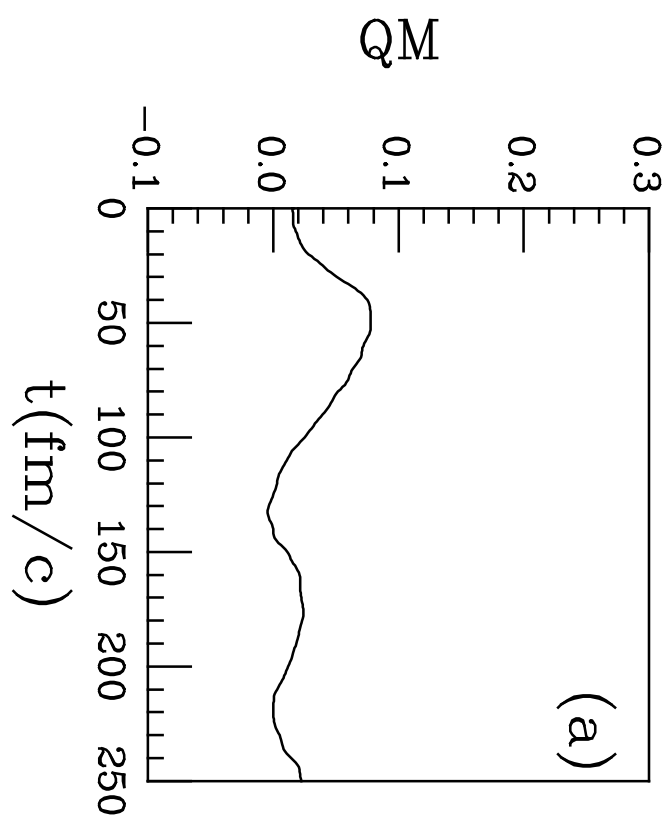
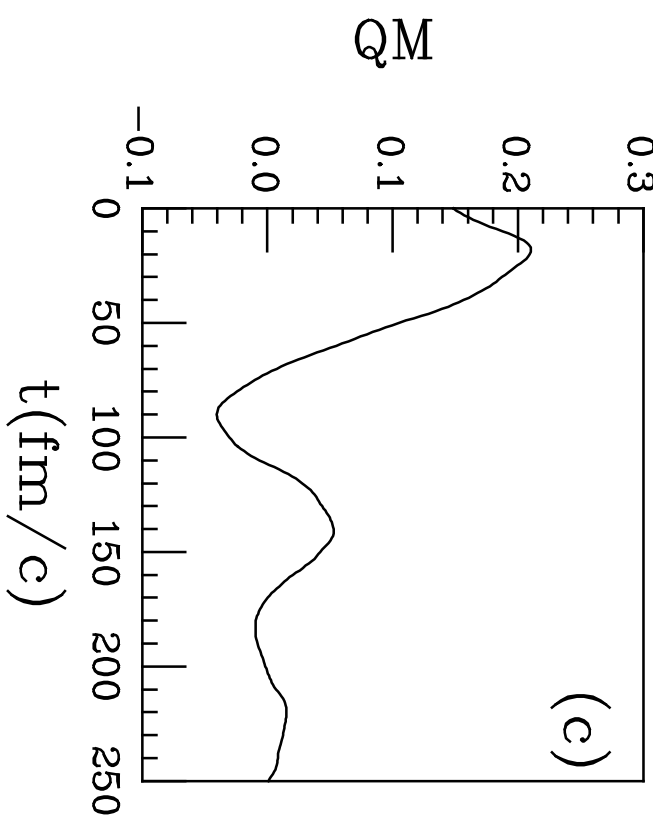




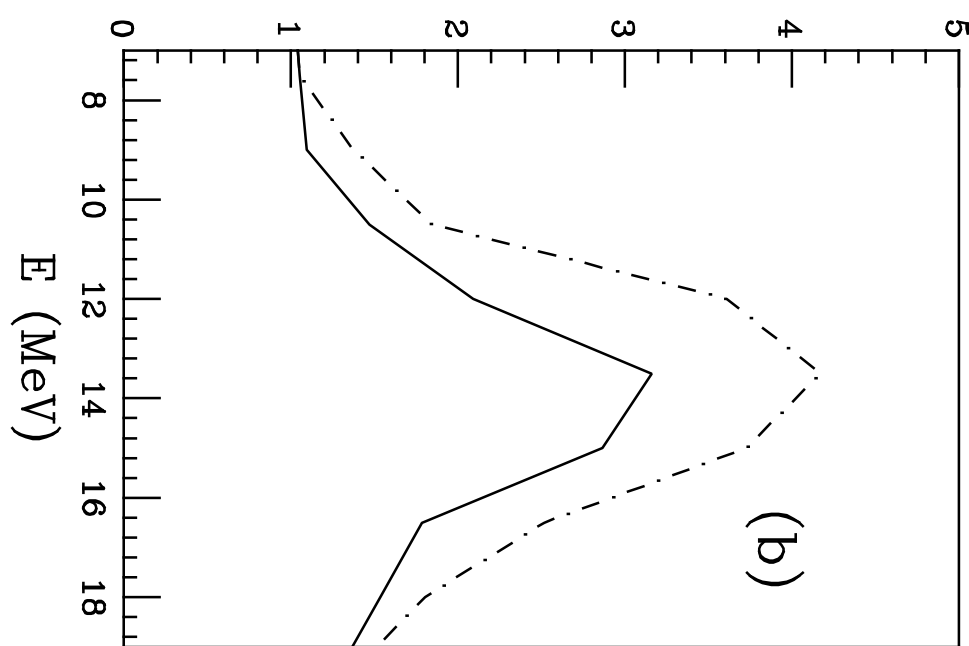
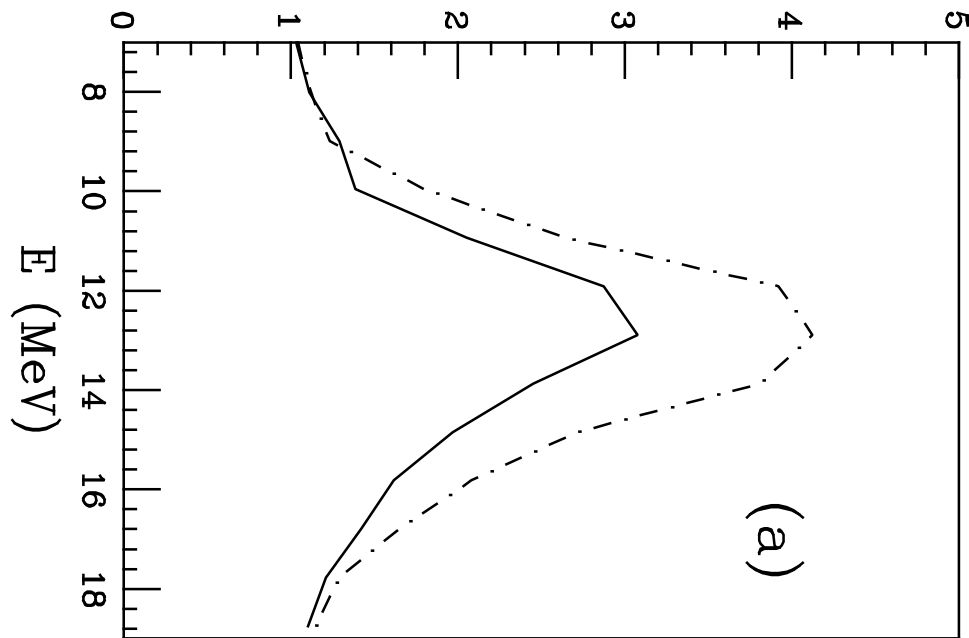




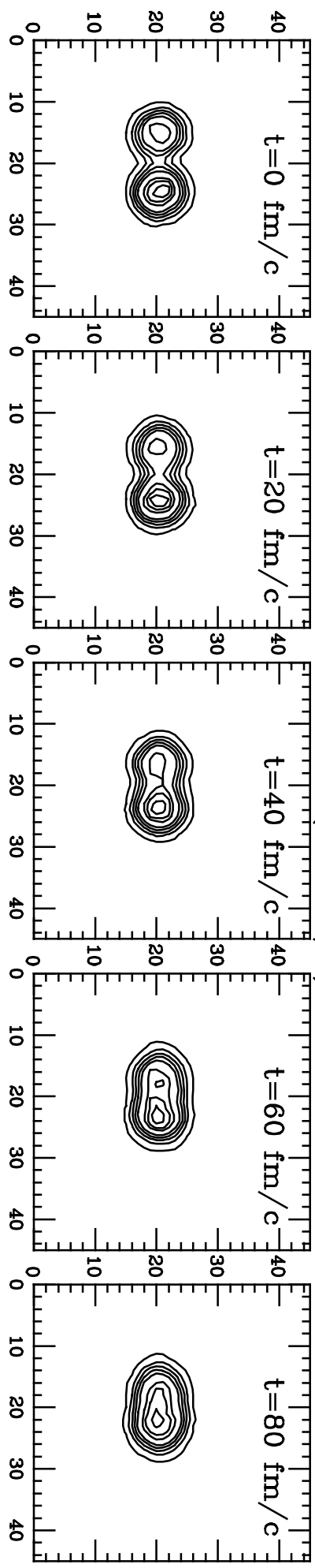




Yields (a.u.)



Cr + Ni (3.5 MeV/n)



Cr + Ni (5.5 MeV/n)

